Journal of Energy Storage 97 (2024) 112706

Contents lists available at ScienceDirect

Journal of Energy Storage

journal homepage: www.elsevier.com/locate/est

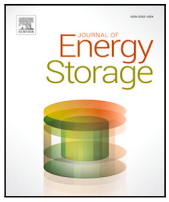

Research papers

Sizing energy storage in electricity grids containing flexible loads

Edmund W. Schaefer [a,b,*], Gerwin Hoogsteen [a], Johann L. Hurink [a], Richard P. van Leeuwen [b]

[a] Department of EEMCS, University of Twente, Enschede, The Netherlands
[b] Department of Sustainable Energy Systems, Saxion UAS, Enschede, The Netherlands

ARTICLE INFO

Keywords:
Electricity grid flexibility
Energy storage sizing
Flexible loads
Electrical vehicle charging
Heat pumps

ABSTRACT

Flexible loads such as EV chargers and heat pumps have the potential to reduce the amount of energy storage required to handle local power imbalances. However, when sizing energy storage these loads are often neglected. Thereby it is unclear how intelligently controlled flexible loads influence energy storage sizing. Therefore, this paper presents an empirical study into the effect of controlling four different classes of flexible loads on energy storage sizing, under which fall existing technologies such as EV chargers, heat pumps and white-goods. We use a Profile Steering control strategy to minimize the power imbalance over the considered period. Furthermore, we use parameter sweeps to investigate the influences of load availability and load demand on the energy storage sizing, and visualize the energy storage reduction with heat maps. The results show that significant energy storage sizing reductions are possible if flexible loads are considered, including a reduction in capacity of more than 60%. Furthermore, if flexible loads can also supply their buffered power to the local microgrid (such as with V2G applications), the need for energy storage is almost completely removed. We conclude that it is important to consider local flexible devices when sizing storage in order to avoid over-dimensioning.

1. Introduction

Electricity grids currently do not provide the capacity needed to handle the mass integration of new devices, which is critical as part of the ongoing energy transition. The mass integration of Renewable Energy Sources (RES) and electrified loads such as Electrical Vehicle (EV) chargers and heat pumps leads to net congestion, whereby the electricity grid's distribution capacity is insufficient to handle local power imbalances in the grid. In the Netherlands, a country with a high quality of electricity supply [1], net congestion has led to a waiting list for the realization of new or upgraded grid capacity connections in recent years [2], which prevents customers on this list from integrating RES and electrified loads. Furthermore, the number of disruptions at transformers has increased dramatically in recent years [3].

Therefore, there is an urgent need to increase the flexibility of the electricity grid. Hereby many definitions of flexibility exist with varying detail [4–6], but in this work we consider flexibility more generally to be a network's ability to match electricity supply and demand under uncertainty [7]. Increases in flexibility are achievable by reinforcing grid infrastructure, such as transformers and cables, by adding Energy Storage Systems (ESS) with one or more control objectives [8], as well as by controlling so called flexible loads [9], which we define as loads whereby the power is controllable over time. Furthermore, integrating properly sized ESS as well as controlling flexible loads can potentially reduce the required grid reinforcement [10,11].

ESS sizing for microgrids is challenging, as many factors can be considered, including available storage technologies, the evolving composition of connected loads, as well as potential ESS control objectives and strategies. Additionally, behaviour of flexible loads connected to the grid affect the ESS requirements needed to remove any grid flexibility deficit. We hypothesize that not considering flexible loads when sizing ESS leads to an increased risk either of over-dimensioning the ESS, resulting in needless extra costs, or under-dimension the ESS, resulting in insufficient local microgrid flexibility. A comprehensive analysis of how considering flexible loads affects ESS sizing is therefore of interest. Finally, an analysis examining the differences between specific types of flexible loads in respect ESS sizing reduction is important, as this leads to more informed microgrid design and operation choices.

1.1. Related work

1.1.1. Control of ESS and flexible loads

Considerable research investigates methods of controlling both ESS as well as flexible loads. In literature, the terms control and scheduling are often used interchangeably, although they do not inherently

* Corresponding author at: Department of Sustainable Energy Systems, Saxion UAS, Enschede, The Netherlands.
E-mail addresses: e.w.schaefer@saxion.nl (E.W. Schaefer), g.hoogsteen@utwente.nl (G. Hoogsteen), j.l.hurink@utwente.nl (J.L. Hurink), r.p.vanleeuwen@saxion.nl (R.P. van Leeuwen).

https://doi.org/10.1016/j.est.2024.112706
Received 9 April 2024; Received in revised form 12 June 2024; Accepted 17 June 2024
Available online 29 June 2024

Nomenclature

Abbreviations

BS	Buffer Shiftable
BSP	Buffer Shiftable Positive
$BSPTS$	Buffer Shiftable Positive Time Shiftable
DR	Demand Response
DSM	Demand Side Management
EP	Energy Potential
ESS	Energy Storage Systems
EV	Electric Vehicle
$MILP$	Mixed Integer Linear Programming
PS	Profile Steering
PV	Photovoltaic
RES	Renewable Energy Sources
TAW	Time Availability Window
TS	Time Shiftable
$V2G$	Vehicle to Grid

List of Symbols

μ	Mean of the distribution
σ	Standard deviation
$\vec{P_{base}}$	Microgrid demand load profile [W]
$\vec{P_d^{FL}}$	Demand load profile of a flexible load, whereby FL is either TS or BSPTS and d is the duration of the load profile in minutes [W]
$\vec{p_d}$	Desired load profile
$\vec{P_{imb}}$	Microgrid imbalance load profile [W]
$\vec{P_{PV}}$	Microgrid production load profile [W]
$\vec{x_d}$	Controllable load profile
E_{cap}^{ESS}	Storage capacity [Wh]
E_{cap}^{FL}	Buffer capacity of a flexible load, whereby FL is either BS, BSP or BSPTS [Wh]
E_{cap}^{FL}	Energy demand of a flexible load over the period, whereby FL is either BS, BSP, TS or BSPTS [Wh]
E_d	Euclidean distance
$E_{imb}(t)$	Microgrid imbalance energy available at time t [Wh]
E_{total}	Total Energy available over the simulation period [Wh]
EP_+	Surplus energy potential [Wh]
EP_-	Deficit energy potential [Wh]
P_{ch}^{ESS}	Storage charge power [W]
P_{dis}^{ESS}	Storage discharge power [W]
P_{max}^{FL}	Maximum power of a flexible load, whereby FL is either BS, BSP, TS or BSPTS [W]
$P_{PV}(t)$	Microgrid production at time t [W]
P_{step}	Power step-size for BSP, BS and BSPTS flexible load types [%]
T_{end}	End time of TAW [hours]
T_{start}	Start time of TAW [hours]

have the same meaning. Control tends to refer to real time decisions, while scheduling refers to actions planned in advance using scheduling algorithms. In this research, we use the term control to describe the act of deciding the action for a component, for example charging or discharging of ESS.

In literature, many Demand Side Management (DSM) approaches have been investigated. [12] provides a comprehensive overview of DSM definitions from literature. For the purposes of this research, we consider DSM to be any and all control actions that are undertaken on the demand side of an electricity grid. This included controlling flexible loads and ESS, as well as locally generated power.

There is a significant body of research which considers DSM strategies that focus on ESS control, while neglecting flexible loads. For example, [13] presents a number of researches conducted into different types of ESS control strategies. The control objectives include stabilizing intermittent (wind) power generation, providing power quality support and providing power balancing support. These researches do not consider controlling local flexible loads, in contrast to [14]. In [15] a comprehensive review of reliability studies pertaining to ESS is given, including an exhaustive list of studies where DSM related to ESS is evaluated. A more general microgrid example with a number of flexible loads is presented in [11], which investigates the effect of controlling a number of flexible loads and ESS as part of a control strategy which aims to make a neighbourhood as autarkic as possible. It is found that adding ESS leads to the largest increase in autarky, even without smart control, while controlling ESS according to a DSM strategy further increases autarky.

When flexible loads are considered in DSM strategies, often a single type of flexible load is considered. EV charging control is often researched, as the integration of EV charges into the electricity grid presents a number of challenges and opportunities [16]. [17] presents a comprehensive review of EV control strategies, including an overview of optimization objectives and methods. The objectives include minimization of peak loads, frequency regulation, cost reduction as well as cost fluctuation minimization. Research often focuses on the advantages of DSM approaches in EV charging in comparison to uncontrolled EV charging. For example, [18] investigates the impact of two EV charging optimization strategies on local EV load shedding as well as feed-in curtailment. Hereby one strategy allows Vehicle to Grid (V2G) charging. The authors find that significant reduction in EV curtailment (between 60%–89%) and small reduction in generated energy curtailment (0.5–1.5%) is possible. Another example is [19], where the authors find a 10%–37% peak reduction in a neighbourhood DSM scenario with an EV and ESS combination. Finally, [20] presents a practical study whereby EVs are charged based on a strategy whereby data is entered by the EV charger users. Applying the strategy achieved an average peak reduction of 48%, even though the data entered by the users was not always accurate.

Besides EVs, heat pumps can also offer flexibility to grids, specifically in residential microgrids. [21] considers controlling a heat pump combined with a thermal storage using a peak reduction strategy, and show that peaks can be reduced but overall energy usage remains the same, while comfort is minimally affected. In further work, [22] considers a case where a price signal is used to control a heat pump to decrease operational costs, and shows that grid peaks are reduced while overall energy consumption is increased. Finally, [23] investigates a multi-zone tariff DSM strategy scenario with a heat pump, PV and ESS, and concludes that a 40% cost reduction is possible.

Finally, there is some research that investigates the advantages of using the flexibility offered by shiftable devices such as white goods. We conclude that this is less prevalent than EV charging and heat pump research. [24] investigates the possible flexibility offered by white goods and EV charging, and concludes that white goods offer only marginal flexibility compared to EV charging and ESS, and surprisingly that the value of EV charging flexibility in certain cases may be higher than that of ESS. Furthermore, [25] presents different DSM approaches

for a case which considers ESS and white goods, thereby modelling both the technical aspects of the microgrid as well as behavioural aspects, whereby a proposed Mixed Integer Linear Program is used to maximize user satisfaction. User satisfaction is quantified based on a Prospect Theory approach [26]. The authors show that ESS is more effective in reducing costs in comparison to white goods, while the white goods are more effective in increasing end-user satisfaction.

In summary, control of flexible loads such as EVs, heat pumps and white goods can potentially reduce power peaks as well as costs. Flexible loads tend to be considered separately in research, and there is a significant portion of research that focuses only on ESS control, neglecting flexible load control. Furthermore, investigations tend to be use case specific, and often overlook comparisons between different flexible loads.

1.1.2. ESS sizing

ESS sizing is prevalent in literature. Both [13,27] present a number of methods and examples for sizing ESS, which include analytical, statistical, mathematical optimization and heuristic based methods. Furthermore, not all research considers DSM when sizing storage. [28] provides an overview of published research which consider optimal sizing of ESS from a more general microgrid perspective, where more than half of the surveyed papers do not consider DSM.

When DSM is considered, much sizing literature investigates DSM approaches which focus on ESS control. [29] presents a two-layered optimization model to investigate an industrial case, focusing on sizing and scheduling optimization, and finds that the proposed method can improve the benefits of ESS. Furthermore, [28] investigates a household scenario considering ESS control, whereby optimization is used to find storage capacities. A scenario is investigated which considers ESS control with a DSM strategy incorporating battery state-of-charge and weather forecasts, and one that does not consider the DSM strategy when controlling the battery. The authors find a storage capacity reduction of 31% when using the DSM approach versus not using it.

Other research considers local flexibility more generally when sizing ESS. [30] presents a Mixed Integer Linear Programming (MILP) method (an often used method for sizing ESS) while also considering the Demand Response (DR) of the available controllable loads. Here, the authors present a comparison of difference ratios of flexible loads in respect to non flexible loads, with no specific type of flexible load chosen. For different scenarios, the authors found that by increasing the amount of flexible loads, the ESS sizing was reduced. Furthermore, [31] presents an investigation into the joint optimal sizing of ESS, PV and wind turbines using an similar MILP approach in a microgrid whereby 10% of loads are shiftable. The authors find that the ESS capacity is reduced by 11%–23% depending on the DR algorithm used.

Further research investigates ESS sizing while considering specific types of flexible loads. [32] uses an MILP based cost optimization for a building use case including both shiftable loads as well as EVs with V2G capabilities, while also considering grid and component limitations. The authors find that their scheme both improves daily operational and trading costs of the EV charging station and reduces reliance on the connected grid. Furthermore, [33] presents an investigation into ESS sizing for a EV charging plaza (no V2G), whereby the ESS was sized directly to limit the usage of the connected grid power through power threshold control. The authors show that already a relatively small ESS sizing can considerably decrease the required grid connection. Also, [34] presents a method for optimally sizing ESS for a grid-connected microgrid with EV charging. The authors find that ESS sizing can be significantly reduced (33%–64%) by controlling EV charging. Furthermore, V2G adoption leads to significant reductions in ESS sizing in comparison to the non-controlled case (56.4%–76%).

Finally, other research focuses on the flexibility provided by heating devices such as heat pumps. [35] investigates a situation whereby a central hydrogen system is sized while considering DR of household heating storage system, and finds a possible 14% hydrogen capacity reduction. Furthermore, [36] investigates possible ESS sizing reductions in a neighbourhood with e-boilers and other shiftable loads which uses DSM, and show ESS capacity decrease on average of 63.71%.

In summary, the advantages of using different types of flexible loads from the perspective of ESS sizing are broadly clear, but tend to be investigated case dependent, whereby load types are not compared. Therefore, a more conceptual investigation into different types of flexible loads is needed, which investigates and compares the influences of key flexible load characteristics on ESS sizing. Such an investigation could be useful in the context of making a broad range of design decisions in energy systems, including choice of flexible load, ESS sizing and electricity grid capacity.

1.2. Main contributions

This paper investigates the potential impacts of different types of flexible loads on the ESS sizing required to handle remaining power imbalances. The goal is to distil generalized insights with which researchers and professionals can approach similar problems when they are investigating more specific case studies. Hereby we focus on the energy aspect in time linked intervals (i.e., causal systems). Furthermore, this paper examines how different flexibility constraints of flexible loads influence the sizing. Note that energy storage is considered to be an enabling technology, and a financial evaluation is not considered.

The main contributions of this paper are:

1. Insights into the effects of using flexible loads on the ESS sizes required to handle power imbalances, including differences between flexible loads.
2. Insights into the fundamental characteristics of flexible loads and how the flexibility offered by a load affects the size of the ESS required to handle a given power imbalance.
3. A method to investigate ESS sizing in relation to the control of flexible loads and corresponding results.

The remainder of the paper is organized as follows. First, Section 2 presents the research method, as well as the used microgrid model and its components, and Section 3 presents the results of the investigation, including an analysis of each type of flexible load. Next, Section 4 provides more general insight into the findings of this research, followed by Section 5 which concludes this paper and details several promising avenues for future work.

2. Method and model

This section presents the method and model used in this research. First, we discuss the different types of flexible loads considered. Then, we present a method used to investigate each type of load. Finally, this section details the model used for each flexible load.

2.1. Flexible loads

In this paper, we consider four different flexible load types (see Table 1). PV curtailment is not considered. Each flexible load type corresponds to a specific existing load type used in residential microgrids, whereby usage is expected to increase as part of the energy transition. Furthermore, we assume that the energy requirement of each flexible load type must be fully met (i.e., no flexible curtailment is possible). A more general relationship diagram is presented in Fig. 1, wherein the various powers and applicable energy capacities are shown. For more on the mathematical models of the various flexible load types, see Appendix.

First, Buffer Shiftable (BS) and Buffer Shiftable Positive (BSP) loads represent EVs connected to chargers. Both BS and BSP types have a Time Availability Window (TAW) and a controllable power demand

Table 1
Overview of flexible load characteristics.

Device type	Practical example	Time Availability Window (TAW)	Demand duration	Internal energy buffer	Buffer usage
Buffer Shiftable Positive (BSP)	EV, no V2G	Adjustable	Adjustable	Yes	Load only
Buffer Shiftable (BS)	EV with V2G	Adjustable	Adjustable	Yes	Load and microgrid
Time Shiftable (TS)	White goods	Adjustable	Constant	No	–
Buffer Shiftable Positive Time Shiftable (BSPTS)	Heat pump	Constant	Adjustable	Yes	Load only

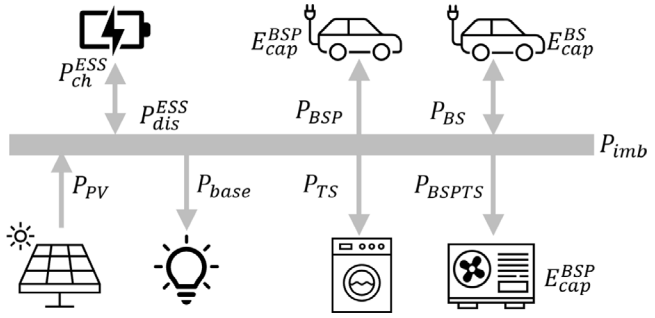

Fig. 1. Relationship diagram between various powers and capacities in the microgrid. Note that in each simulation only one flexible load (BSP, BS, TS or BSPTS) is evaluated at a time.

within the given TAW. We define a TAW as a time interval in which the flexible load is available for controlled usage. Furthermore, both BS and BSP types allow for internal energy buffering, enabling a wide degree of freedom to compose load profiles within a given TAW. A BS differs from a BSP in its possible interactions with a connected microgrid: a BS can discharge internally buffered energy into a connected microgrid (so called V2G), whereas a BSP can only act as a load.

Next, Time Shiftable (TS) loads represent white goods such as washing machines and dishwashers. These appliances have a fixed load profile that cannot be interrupted. Furthermore, in contrast to both BS and BSP types, energy cannot be locally buffered. However, the load profile is shiftable within a given TAW without a significant decline in user comfort.

Finally, Buffer Shiftable Positive Time Shiftable (BSPTS) loads represent heating devices such as heat pumps and e-boilers. These devices are always connected to the grid (and thus we consider them to have no TAW) and can buffer energy, but in a different form than electricity (heat). This implies that internally buffered energy cannot be discharged to a connected microgrid. Furthermore, BSPTS loads are supplied from their internal buffer which can be pre-filled, enabling a wide degree of freedom to compose load profiles within a given TAW.

2.2. Method

To evaluate the effect of flexible load control on the sizing of a microgrid ESS, a control strategy is required. We choose a Profile Steering (PS) based approach and solution method [37]. To work, this approach requires schedules from each device that adhere to the constraints of that specific device. Each of these profiles is optimized based on a given input, namely a derived energy profile. For this we use the tailor made optimization algorithms presented by [38]. These profiles are then aggregated by a higher-level coordinator in the PS heuristic. The PS algorithm then selects from all of the received device profiles, the device that contributes the most to the overall objective of peak-shaving. Subsequently, the desired profile for the other devices is updated, thereby including the influence of the selected profile. These steps are repeated until there is not sufficient improvement, thereby finding the Euclidean distance E_d between a desired load profile $\vec{p}$ and the controllable load profile $\vec{x}$ (see Eq. (1) from [37]). We select PS both because it inherently keeps as much energy as possible local (which corresponds to the aim of this research) as well as because it has been proven to be a proper strategy in previous research.

$$E_d = \|\vec{x} - \vec{p}\|_2 \tag{1}$$

In PS, a central controller evaluates bid-in load profiles spanning multiple time intervals from flexible loads and other available flexible components. Then, the controller accepts the best bid for its purpose (i.e., the profile that reduces E_d the most) and rejects the others. The central controller repeats the process until E_d is not longer reduced. Within this research we select a zero profile for $\vec{p}$ which supports self sufficiency of the considered case, as the PS algorithm attempts to minimize the microgrid imbalance using the connected flexible loads. Furthermore, as any remaining power imbalance ($\vec{P_{imb}}$) cannot be handled by the set of flexible loads, it must be handled by the ESS. [37] presents a more detailed description of the PS algorithm as well as several use cases. [11] presents a practical PS neighbourhood use case containing a heat buffer, and [20,39] present EV charging scheduling with PS. An open source software implementation of PS is available at [40].

Based on the final imbalance profile $\vec{P_{imb}}$ found through the PS algorithm, ESS requirements are derived using the approach presented in [41], specifically the storage capacity (E_{cap}^{ESS}), the maximum charge power (P_{ch}^{ESS}) and the maximum discharge power (P_{dis}^{ESS}). Hereby, the ESS is considered to be ideal, as technology dependent constraints such as charge and discharge efficiency as well as self-discharge are not considered in this research.

As each flexible load has several variable parameters, we conduct parameters sweeps of the parameters considered most important (specifically TAW and power based parameters). These sweeps provide insights into how these parameters influence sizing of the microgrid ESS. Each type of flexible load has its own characteristics as presented in Table 1. In Section 3 we examine per flexible load type which parameters can be varied. To be able to give proper insights we use heat maps to visualize certain data. Hereby all possible TAWs investigated in each parameter sweep are shown, while line-graphs and tables are more useful when only a sub-set of TAWs are visualized.

2.3. Microgrid model and simulation

To gain insights into the effects of flexible loads on ESS sizing, we first select a stylized microgrid case for evaluation. Hereby we choose a straightforward base-load and generation model to be able to gain deeper insights into the core contributions that flexible loads can provide when sizing ESS.

A simulation period of 24 h (1440 min) is selected, as day/night cycles are leading in grids with a high penetration of PV as well as in residential grids which often contain the types of flexible loads under investigation. As we are mainly focusing on energy aspects, we discretize the time horizon in time intervals 1, …,T. A value for a time interval $t \in 1, \ldots, T$ specifies the energy content for that interval. Intervals of 1 min are used to provide confidence that the found ESS sizing is reliable, as demonstrated in [42]. Furthermore, this research considers each TAW period to be in multiples of fifteen minutes to reduce the computational time of the parameter sweeps, while still ensuring insights can be gained. Finally, the used PS control objective is chosen to be to reduce any power imbalance to zero, which corresponds to the objective of local peak reduction.

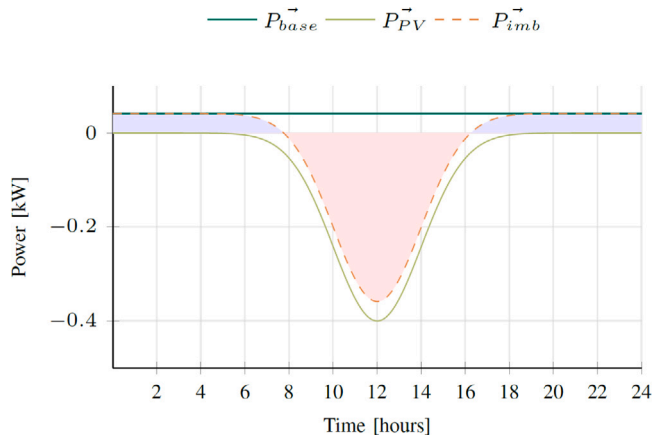

Fig. 2. P_{PV}, P_{base} and P_{imb} profiles over 24 h period. (For interpretation of the references to colour in this figure legend, the reader is referred to the web version of this article.)

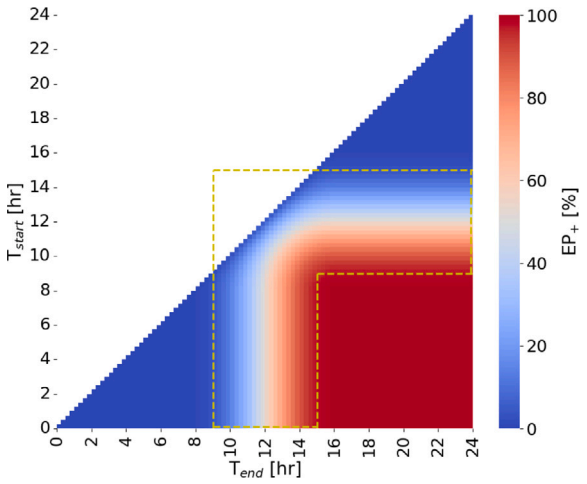

Fig. 3. Microgrid EP_+.

The microgrid case contains both a production component P_{PV} and a non-flexible load component P_{base}, which together specify the imbalance of the microgrid P_{imb}. P_{imb} has both positive and negative values over the simulation period, whereby positive power values indicate power demand and negative power values indicate power production. The sum of all energy demand and production in the microgrid over the simulation period, including the flexible load, is chosen to be 0 kWh, which ensures that it is energetically possible to find a solution in each case. Buffers are initialized empty to ensure no extra energy is introduced into the microgrid.

For P_{base} a constant power profile over the simulation period is chosen, meaning that the profile is flat. For P_{PV} we use an artificial PV generation profile P_{PV} which together with the static base-load demand profile P_{base} creates the profile P_{imb} (Fig. 2). Concretely, we create a Bell-curve to represent P_{PV} using Gaussian distribution (Eq. (2) from [43]), whereby σ is the standard deviation, μ is the mean of the distribution [43]. We do not consider other PV profiles such as those effected by adverse weather conditions, as this study focuses on the (generalized) maximum storage required to shift the energy from production to demand.

$$P_{PV}(t) = \frac{1}{\sigma * \sqrt{2\pi}} * e^{-\frac{1}{2}*(\frac{t-\mu}{\sigma})^2} \tag{2}$$

3. Results and analysis

This section details the energy potential for the selected microgrid situation and the results of the investigations for the different flexible loads. Hereby for each flexible load the used parameters, expectations, simulation results and a short reflection is presented.

3.1. Energy potential

Before analysing the results of the parameter sweeps, we first consider the distribution of the imbalance energy within the microgrid without the flexible load (i.e., only P_{base} and P_{PV}) . This provides insight into how much energy should ideally be shifted by the flexible loads. First, Eq. (3) shows the percentage of the amount of energy that is available within a given TAW in respect to the total energy available within the evaluation period, which we call Energy Potential (EP). Hereby T_{start} is the TAW start interval, T_{end} is the TAW end interval, $E_{imb}(t)$ is the energy imbalance at interval t and E_{total} is the total energy available within the simulation period.

$$EP = \frac{1}{E_{total}} \sum_{t=T_{start}}^{T_{end}} E_{imb}(t) \tag{3}$$

The value EP for a TAW specifies the relative energy amount of the TAW. For the following analysis we also need the relative positive and the relative negative energy in a TAW. For this, by EP_+ ($EP\_$) we denote the total positive (negative) energy within the TAW; i.e., we add up the values $\max(E_{imb}(t), 0)$ ($\min(E_{imb}(t), 0)$) over all time intervals t in the TAW, and normalize this sum by the sum of the total positive (negative) energy of the simulation period. EP_+ represents local overproduction and requires flexibility whereby energy can be absorbed, and $EP\_$ represents local underproduction and requires flexibility whereby energy can be distributed. Evaluation of both $EP+$ and $EP\_$ is done separately, as they both relate to different flexibility requirements from a flexible load. Furthermore, note that the imbalance vector P_{imb} of a TAW may contain in some parts an energy surplus and in other parts an energy deficit.

As previously mentioned, we use heat maps to visualize data to give overviews of EP values over all possible TAWs. Hereby the EP values for all possible TAWs based on a specific TAW $[T_{start}, T_{end}]$ are given, whereby the points corresponding to T_{start} are given on the y-axis and the points corresponding to T_{end} are given on the x-axis. Thereby, trends between TAWs can be identified by examining the surrounding area.

Fig. 3 shows the EP_+ heat map for the considered microgrid. As previously stated, only P_{base} and P_{PV} are included. The maximum possible EP_+ is equal to the aggregated energy content of the red area of P_{imb} in Fig. 2 i.e., the total amount of surplus energy available during the simulation period. In Fig. 3, the EP_+ values for the TAW interval are presented by colours. The dark blue colour represents TAWs where (almost) no surplus energy is available to be used by a flexible load, and the dark red colour represents TAWs where (almost) all surplus energy is available. In reference to Fig. 2, the EP presented in one cell in Fig. 3 with a begin and end time corresponds to the total energy in the red area within the same time interval in Fig. 2. Furthermore, the yellow dashed box in Fig. 3 contains the TAWs which only include part of the energy of the red area in Fig. 2, visualized in Fig. 3 as a shift from blue to red. Furthermore, TAWs with a T_{start} before or at 11:00 and a T_{end} after or at 13:00 contain large EP_+ amounts, and therefore contain the most shiftable energy for flexible loads.

Fig. 4 shows the corresponding $EP\_$ heat map for the considered microgrid. The maximum possible $EP\_$ is equal to the aggregated energy content of the blue area of P_{imb} in Fig. 2 i.e., the total amount of deficit energy available during the simulation period. In Fig. 4 we see that the largest $EP\_$ values are at the bottom right corner of the heat map. This corresponds to the longer TAWs over the total 24 h period. This is because $EP\_$ is based on P_{imb} and more specifically P_{base}, which is evenly distributed over the 24 h simulation period. Note, that TAWs whereby T_{start} is after or at 8:00 and T_{end} is before or at 16:00 do not

Table 2
BSP ESS requirements ranges.

	E_{cap}^{ESS}			P_{ch}^{ESS}			P_{dis}^{ESS}		
	Range (Wh)	Average (Wh)	Max Red (%)	Range (W)	Average (W)	Max Red (%)	Range (W)	Average (W)	Max Red (%)
100%	910–1579	1164	42.35	358–359	358	0.24	3642–4042	3775	9.88
50%	821–1579	1117	47.99	355–359	357	0.98	1645–4042	1824	59.31
25%	646–1579	1031	59.11	345–359	352	3.66	654–4042	902	83.83
10%	579–1579	1000	63.33	286–359	327	20.28	112–4042	442	97.22
4%	579–1579	1000	63.33	165–359	282	54.00	42–4042	351	98.97
2%	579–1579	1000	63.33	117–359	267	67.63	42–4042	326	98.97
1%	579–1579	1000	63.33	101–359	262	71.75	42–4042	317	98.97

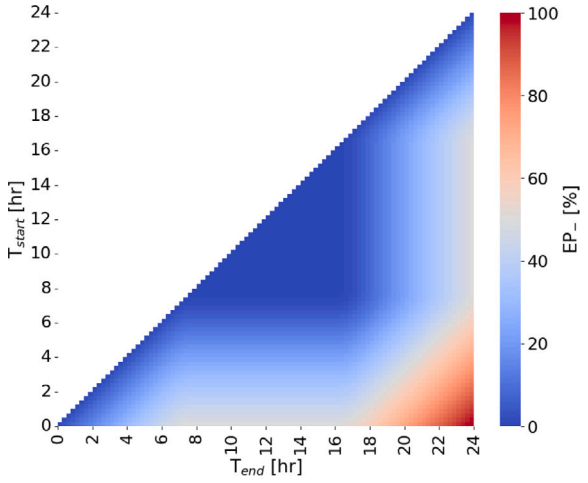

Fig. 4. Microgrid EP_{-}.

lead to larger EP_{-} values, as $\vec{P_{PV}}$ is larger than the baseload $\vec{P_{base}}$ at those intervals (i.e., there is no blue area in Fig. 2).

3.2. Buffer Shiftable Positive (BSP) flexibility

3.2.1. Parameters

The BSP flexible load includes six variable parameters. We vary three of these in two layers of parameter sweeps. First, we vary the TAW start time T_{start} and TAW end time T_{end} to see the influence of BSP availability on ESS sizing. Hereby T_{end} is between 15 and 1440 min (one day), in increments of 15 min. Second, we vary the BSP power step-size P_{step} which specifies the percentage increments of the maximum BSP power P_{max}^{BSP}, to see the influence of BSP controllability on ESS sizing. The step sizes are 100% (on-off functionality only), 50%, 25%, 10%, 4%, 2% and 1% of P_{max}^{BSP}.

The three remaining parameters stay constant. The total energy demand E_{dem}^{BSP} is chosen to be 1 kWh (the total energy demand of $\vec{P_{base}}$ is also 1 kWh). The PV production $\vec{P_{PV}}$ is 2 kWh. This ensures equal energy demand and production over the simulation period. The capacity of the BSP buffer E_{cap}^{BSP} is chosen equal to the E_{dem}^{BSP}. P_{max}^{BSP} is set to 4 kW, to ensure the BSP buffer can be fully charged within the minimum TA.

3.2.2. Expectations

In line with the findings in Section 1.1 and related to [34], by choosing a TAW which overlaps with large EP_{+} moments, we expect the capacity E_{cap}^{ESS} required to decrease, as the BSP is available to shift more energy, thereby requiring less energy to be shifted by the ESS. As the BSP allows for a quick buffering, we expect the decrease of the sizing to be significant. Furthermore, by decreasing P_{step}, the required power P_{ch}^{ESS} will also decrease as P_{ch}^{ESS} is defined primarily by the demand of the BSP ($\vec{P_{base}}$ is much lower than P_{max}^{BSP}).

3.2.3. Results

First, we investigate the influence of P_{step} on the ESS requirements capacity (E_{cap}^{ESS}), charge power(P_{ch}^{ESS}) and discharge power (P_{dis}^{ESS}). Table 2 shows an overview of the ranges of ESS requirements, averages and maximum reduction percentages (Max Red % in Table 2) for all TAWs for each P_{step}. The maximum reductions are in respect to largest ESS sizing required across the simulation period, i.e., the TAW which needs the largest ESS sizing. For these cases, controlling a BSP can reduce E_{cap}^{ESS} up to 42.35% with only on-off functionality. The reduction increases to 63.33% for lower P_{step} values, whereby no further increase is possible for values lower than 10%. Therefore, depending on the TAW, any control of a BSP with any P_{step} can allow for a significant reduction in maximum E_{cap}^{ESS}.

To be able to reduce P_{dis}^{ESS} by more than 10%, the BSP needs a P_{step} of at least 50%. Furthermore, a P_{step} of 10% or lower leads to a 97%–99% reduction. In comparison, P_{ch}^{ESS} requires at least a P_{step} of 4% for significant reductions. Note that the ratios between P_{dis}^{ESS} and P_{ch}^{ESS} in absolute terms differ significantly depending on P_{step}, whereby for a P_{step} of 25% and higher the maximum P_{dis}^{ESS} is around 2–10 times larger than the maximum P_{ch}^{ESS}. The power value which is higher for any TAW (either P_{ch}^{ESS} or P_{dis}^{ESS}) is generally leading when specifying ESS sizing. Depending on the TAW, step sizes P_{step} of 10% or lower leads to comparable orders of magnitude between P_{ch}^{ESS} and P_{dis}^{ESS}.

Next, we investigate the influence of the TAW on the ESS requirements, whereby for P_{step} we focus on values of 1% and 100%, which provide the most (Fig. 5) and least (Fig. 6) flexibility respectively. Both Figs. 5 and 6 show square shaped windows that are comparable to large surplus energy (EP_{+}) moments (see Fig. 3). When P_{step} is 100%, the maximum E_{cap}^{ESS} reduction is achieved for all TAWs which include 11:45 h–12:15 h (i.e., E_{cap}^{BSP} is charged at 11:45 or 12:00 h or both), whereby any further widening of the TAW will not reduce E_{cap}^{ESS}. When P_{step} is 1%, the corresponding period is from 11:15–12:45 h, i.e. one hour longer. Furthermore, for both P_{step} values, a TAW within the period from around 11 h to 13 h will already allow for a significant reduction of E_{cap}^{ESS} of between 33.4% and 42.3%.

Fig. 7 shows the maximum charge power P_{ch}^{ESS} reductions for a P_{step} of 1% (100% is not shown as the possible P_{ch}^{ESS} reduction is small, see Table 2), for the same TAWs as in Fig. 6. However, the corresponding window size is narrower for maximum P_{ch}^{ESS} reduction, meaning the TAW must include a larger period (between 9 and 15 h) to achieve maximum P_{ch}^{ESS} reduction.

For the maximum discharge power P_{dis}^{ESS}, a P_{step} of 100% does not allow for much reduction, but at 1% larger decreases are possible across all TAWs of 30 min or longer (see Fig. 8). Furthermore, all TAWs of 45 min or more enable a maximum P_{dis}^{ESS} decrease of at least 49.48%, which further increases to 75.22% if the TAW is at least one hour.

3.2.4. Reflection

The results of the simulation confirm expectations prior to testing, and are comparable to the findings in [34]. However, the influence of P_{step} was not expected to be that large, especially with respect to E_{cap}^{ESS}. When using a BSP flexible load, a P_{step} of 10% is already enough to significantly decrease all ESS requirements in combination TAWs with a large EP_{+} (large surplus energy to utilize). Finally, additional

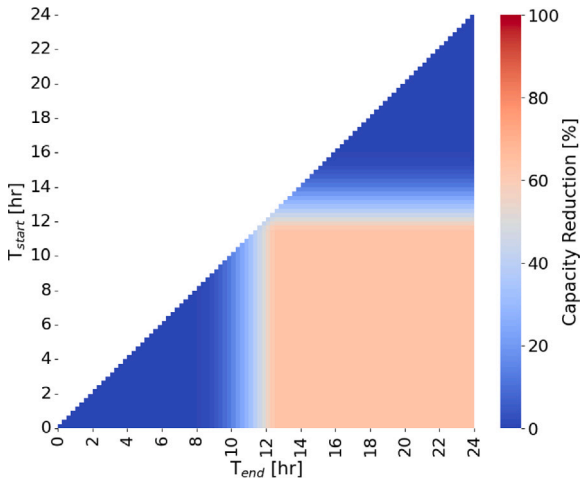

Fig. 5. BSP: E_{cap}^{ESS} per TAW, P_{step} = 1%.

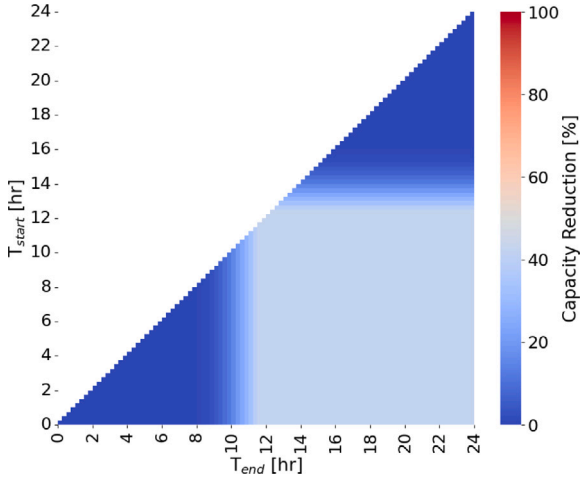

Fig. 6. BSP: E_{cap}^{ESS} per TAW, P_{step} = 100%.

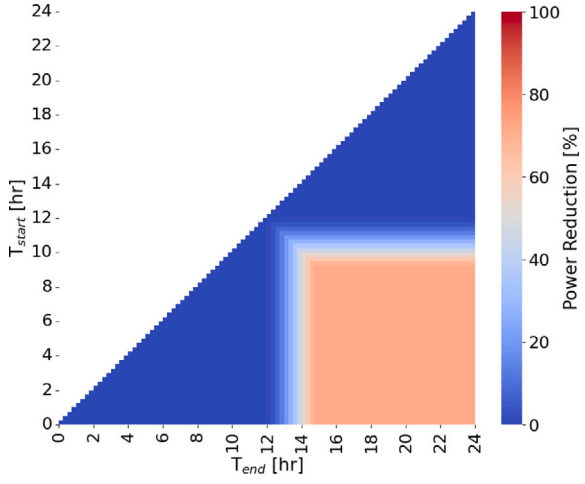

Fig. 7. BSP: P_{ch}^{ESS} per TAW, P_{step} = 1%.

availability outside of the large EP_+ moments will not decrease the ESS requirements further, but including at least a part of a large EP_+ moments will decrease ESS requirements considerably. This confirms

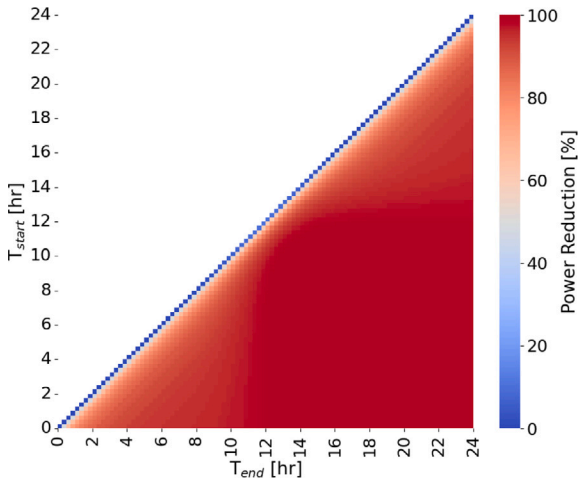

Fig. 8. BSP: P_{dis}^{ESS} per TAW, P_{step} = 1%.

the findings in [20] that TAWs can be quite flexible and have a significant impact on peak reduction.

3.3. Buffer Shiftable (BS) flexibility

3.3.1. Parameters

The BS has the same six parameters as the BSP. For these simulations, all parameters are chosen to be the same as in the BSP simulations, except P_{step}, which can now also be a negative value (power discharge). We vary P_{step} with the same percentages as for BSP, but also with the negative values, i.e., P_{step} = 100% means that P_{max}^{BS} is possible both for charging as well as discharging, and also that the BS can have no power exchange (0 W).

3.3.2. Expectations

Compared to the BSP results, we expect a BS to enable further capacity E_{cap}^{ESS} decreases, as found in [34], specifically when TAWs are longer. This further reduction is due to the BS functioning more as storage and it being available to serve energy required by $\vec{P_{base}}$. Furthermore, we expect comparable reductions of maximum charge power values P_{ch}^{ESS} and maximum discharge power values P_{dis}^{ESS} with respect to the BSP, as the BS discharge can only serve $\vec{P_{base}}$, which demands low power relative to the BS demand.

3.3.3. Results

We first investigate the influence of P_{step} on the ESS requirements E_{cap}^{ESS}, P_{ch}^{ESS} and P_{dis}^{ESS} (see Table 3). As with the BSP, the maximum reductions are in respect to largest ESS sizing required across the simulation period. For all ESS requirements where P_{step} is 10% and larger, the values are identical to the BSP case. However, further maximum reductions in comparison to a BSP are possible for P_{step} values of 4% and smaller, as the BS must be able to discharge a small enough power value to service $\vec{P_{base}}$. When P_{step} is 1%, the ESS requirements can be reduced to 94%–99% in respect to the maximum required sizing. Using BS flexibility can therefore almost completely remove the need for any ESS if the TAW is sufficiently long (i.e., almost the entire day).

As with the BSP, again we investigate P_{step} values of 100% and 1%. As previously discussed, for larger P_{step} values there are no differences between the ESS requirements when using a BSP or a BS, and therefore the $P_{100\%}$ heatmaps are the same as in Section 3.2. Furthermore, there is a negligible improvement in the maximum P_{dis}^{ESS} reduction when using a BS in respect to a BSP.

Conversely, the E_{cap}^{ESS} (Fig. 9) and P_{ch}^{ESS} (Fig. 10) heat maps do differ. In both figures, the large EP_+ moments are not as clearly visible

Table 3
BS ESS requirements.

	E_{cap}^{ESS}			P_{ch}^{ESS}			P_{dis}^{ESS}		
	Range (Wh)	Average (Wh)	Max Red (%)	Range (W)	Average (W)	Max Red (%)	Range (W)	Average (W)	Max Red (%)
100%	910–1579	1164	42.35	358–359	358	0.24	3642–4042	3775	9.88
50%	821–1579	1117	47.99	355–359	357	0.98	1645–4042	1824	59.31
25%	646–1579	1031	59.11	345–359	352	3.66	654–4042	902	83.83
10%	579–1579	1000	63.33	286–359	327	20.28	112–4042	442	97.22
4%	288–1579	938	81.73	118–359	269	67.00	42–4042	352	98.97
2%	133–1579	922	91.61	38–359	251	89.30	42–4042	327	98.97
1%	16–1579	919	98.98	21–359	247	94.20	19–4042	317	99.53

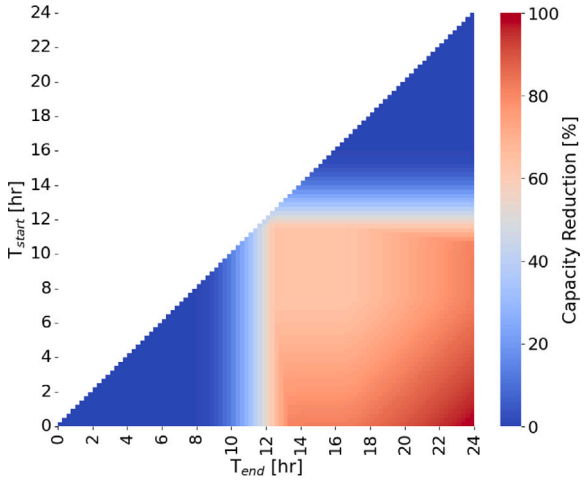

Fig. 9. BS: E_{cap}^{ESS} per TAW, P_{step} = 1%.

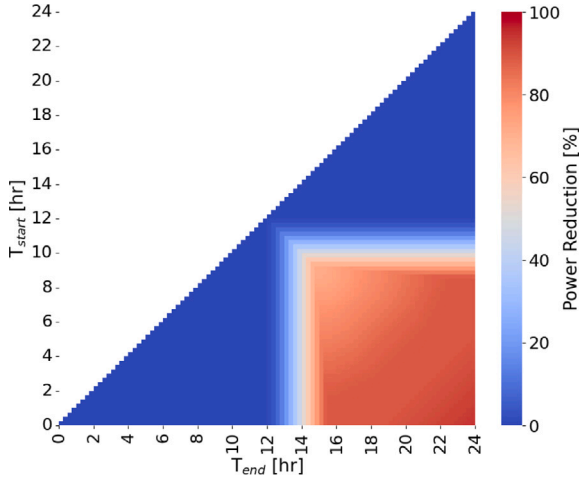

Fig. 10. BSP: P_{ch}^{ESS} per TAW, P_{step} = 1%.

as in the BSP case. This is because EP_{-} influences the ESS requirements due to the BS being available to handle the demand part of $\vec{P_{imb}}$. The E_{cap}^{ESS} and P_{ch}^{ESS} reductions for TAWs which start earlier are lower than for the BSP case if these TAWs stop at around 12 h. Furthermore, the maximum possible reduction is now only available for the longest TAWs, thereby effecting E_{cap}^{ESS} more than P_{ch}^{ESS}. Therefore, in contrast to the BSP, more availability outside of the largest EP_{+} window enables further E_{cap}^{ESS} and P_{ch}^{ESS} reductions.

3.3.4. Reflection

The results broadly confirm expectations prior to testing, but the sizing reductions are higher than in [34]. However, the variance of TAWs starting earlier and lasting until around 12 h was also not expected. Furthermore, we did not expect that the need for ESS would almost be completely removed by using a BS, as it was assumed that the BS alone would not be sufficient to bridge the flexibility gap. Considering EVs, this indicates that V2G could be useful if the vehicle would be available both during large EP_{+} and large EP_{-} moments. However, this usefulness is less robust, as TAW timing and power step-size in relation to $\vec{P_{imb}}$ are critical for additional ESS reductions in this case.

3.4. Time Shiftable (TS) flexibility

3.4.1. Parameters

The TS flexible load includes three parameters, all of which are varied. First, we vary the input load profile $\vec{P_d^{TS}}$ (hereby d is the length of the profile in minutes). Five profiles are created, with a duration of 15, 60, 180, 360 or 720 min. Each profile operates at a constant power P_{max}^{TS}, such that each profile's total energy demand E_{dem}^{TS} equals 1kWh (i.e., the same load as the other flexible loads). Varying the length of the profile while keeping E_{dem}^{TS} constant allows for a comparison of shorter profiles that emphasizes power and longer profiles that emphasize energy.

Second, as in the previous case with flexible loads, we vary T_{start} and T_{end}, to see the effect of TS availability on ESS sizing. Note that for profiles with a duration of 60 min or longer, fewer valid T_{start} and T_{end} values exist compared to previous flexible loads, as the TAW length must at least be equal to the length of $\vec{P_d^{TS}}$, to ensure all energy is served.

3.4.2. Expectations

When a TAW overlaps with a large EP_{+} moment, the maximum required E_{cap}^{ESS} will decrease for all $\vec{P_d^{TS}}$ profiles, but we expect a lower decrease than in most of the BS and BSP situations, as the TS offers less flexibility due to the static $\vec{P_d^{TS}}$ profiles (found in [24]). Similarly the maximum required P_{dis}^{ESS} will decrease, but the absolute decrease itself will be positively correlated to the power demand of $\vec{P_d^{TS}}$.

3.4.3. Results

First, we investigate the influence of the input profiles on the ESS requirements. Table 4 shows the ranges of ESS requirements, maximum reduction percentages and their averages for each input profile $\vec{P_d^{TS}}$. The maximum reductions are reductions in respect to largest ESS sizing required per input profile across the simulation period. In Table 4, we see that using a TS can lead to capacity (E_{cap}^{ESS}) reductions of 23.21% to 63.33%, with a maximum reduction possible for input profiles $\vec{P_{180}^{TS}}$ and $\vec{P_{360}^{TS}}$. The TS case allows similar E_{cap}^{ESS} ranges to the BSP case for most input profiles, with the exception of when $\vec{P_{720}^{TS}}$ is the input profile, as then the maximum of the E_{cap}^{ESS} range is lower than with the other input profiles, and the minimum is higher. This results from $\vec{P_{720}^{TS}}$ being so large there are fewer TAW options, and the given options fit less well within $\vec{P_{PV}}$.

Furthermore, a TS will allow for a reduction of the maximum discharge power P_{dis}^{ESS} of 3.56% to 80.57%, whereby the highest possible

Table 4
TS ESS requirements.

	E_{cap}^{ESS}			P_{ch}^{ESS}			P_{dis}^{ESS}		
	Range (Wh)	Average (Wh)	Max Red (%)	Range (W)	Average (W)	Max Red (%)	Range (W)	Average (W)	Max Red (%)
$P_{15}^{\vec{TS}}$	910–1579	1164	42.35	358–359	358	0.24	3642–4042	3802	9.88
$P_{60}^{\vec{TS}}$	646–1579	1002	59.11	345–359	352	3.66	654–1042	789	37.24
$P_{180}^{\vec{TS}}$	579–1579	885	63.33	259–359	304	27.89	73–375	188	80.57
$P_{360}^{\vec{TS}}$	579–1579	820	63.33	192–359	248	46.48	78–208	131	62.38
$P_{720}^{\vec{TS}}$	984–1281	1005	23.21	275–359	277	23.24	121–125	122	3.56

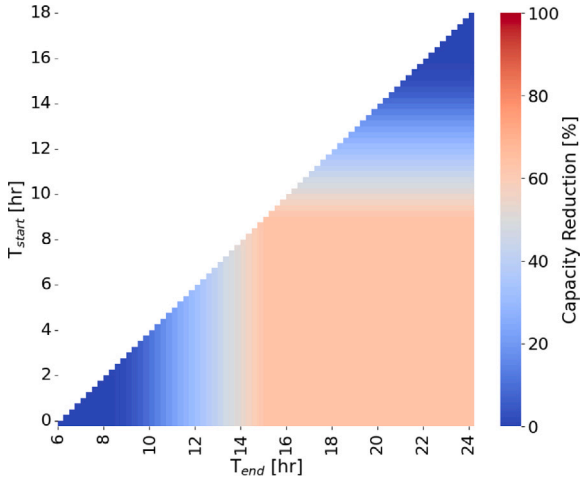

Fig. 11. TS: E_{cap}^{ESS} per TAW, $P_{360}^{\vec{TS}}$.

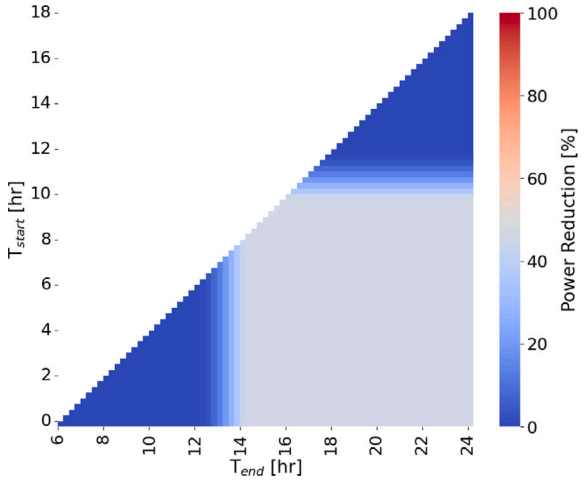

Fig. 12. TS: P_{ch}^{ESS} per TAW, $P_{360}^{\vec{TS}}$.

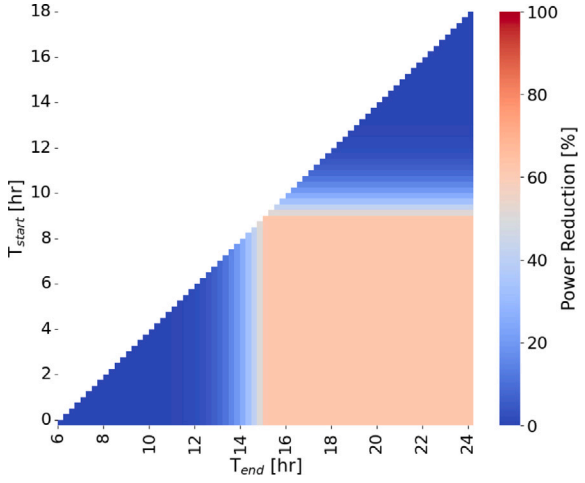

Fig. 13. TS: P_{dis}^{ESS} per TAW, $P_{360}^{\vec{TS}}$.

reduction is with input profile $P_{180}^{\vec{TS}}$. Note that the maximum of the P_{dis}^{ESS} ranges decreases linearly with the decrease in power demand from $P_{d}^{\vec{TS}}$ when also considering the demand of $P_{base}^{\vec{}}$. Last, a TS will allow for a reduction of maximum charge power P_{ch}^{ESS} of 0.24% to 46.48%, with negligible reductions with input profiles $P_{15}^{\vec{TS}}$ and $P_{60}^{\vec{TS}}$. Based on the observations discussed, we conclude that a TS with a $P_{360}^{\vec{TS}}$ profile offers the most flexibility, and therefore allows for the highest possible reductions of ESS requirements when TAWs align with large $EP+$ moments.

Next, we investigate the influences of TAWs on the ESS requirements, whereby we select $P_{360}^{\vec{TS}}$ as input profile for further analysis. Figs. 11–13 show the heatmaps of the ESS requirements E_{cap}^{ESS}, P_{ch}^{ESS} and P_{dis}^{ESS} respectively. Here, maximum windows are visible similar to those seen in the BSP case, corresponding to large EP_{+} moments. The highest reductions of both E_{cap}^{ESS} and P_{dis}^{ESS} are possible for cases where TAWs include the period between 9:00 and 15:00, while the highest P_{ch}^{ESS} reductions are possible for cases where TAWs include fewer hours in the period between 8:00 and 17:00. Furthermore, we see that E_{cap}^{ESS} leads to a more gradual shift for reduction in the TAWs surrounding the maximum window (broader light blue and cream area), while P_{ch}^{ESS} and P_{dis}^{ESS} shifts are less gradual, meaning that the TAW must include as much as possible of the large surplus energy period to achieve significant ESS P_{ch}^{ESS} and P_{dis}^{ESS} reductions.

3.4.4. Reflection

The maximum P_{ch}^{ESS} and P_{dis}^{ESS} decrease was indeed lower than both the BSP and the BS situation, and P_{dis}^{ESS} decreased as expected, and broadly confirming the findings in [24]. Furthermore, we found comparable maximum E_{cap}^{ESS} reductions for input profiles of $P_{180}^{\vec{TS}}$ and $P_{360}^{\vec{TS}}$. Also the range of possible E_{cap}^{ESS} values was the smallest for the longest and least power demanding profile, $P_{720}^{\vec{TS}}$, whereby the maximum of the range differs from the other profiles due to the profile being so long that is always intersects with large EP_{+} TAWs. Finally, we found that it was better to have longer profiles which line up more with EP_{+} availability.

3.5. Buffer Shiftable Positive Time Shiftable (BSPTS) flexibility

3.5.1. Parameters

The BSPTS includes four parameters, two of which we vary with parameters sweeps. First, we vary the input load profile $P_{d}^{\vec{BSPTS}}$ to investigate the effect of different power demands on the ESS requirements. We use the same input load profiles as Section 3.4, whereby the starting time of the profile is varied in increments of 15 min, and the required power of the BSPTS at all moments outside of the profile is

Table 5
BSPTS ESS requirements for $\vec{P_{low}}$ and $\vec{P_{high}}$.

		E_{cap}^{ESS}			P_{ch}^{ESS}			P_{dis}^{ESS}		
		Range (Wh)	Average (Wh)	Max Red (%)	Range (W)	Average (W)	Max Red (%)	Range (W)	Average (W)	Max Red (%)
P_{low}	$P_{15}^{\vec{BSPTS}}$	910–1579	1198	42.35	358–359	358	0.24	3642–4042	3802	9.88
	$P_{60}^{\vec{BSPTS}}$	646–1579	1451	59.11	345–359	358	3.66	654–1042	972	37.24
	$P_{180}^{\vec{BSPTS}}$	579–1579	1346	63.33	259–359	354	27.89	73–375	332	80.57
	$P_{360}^{\vec{BSPTS}}$	579–1579	1236	63.33	192–359	327	46.48	78–208	194	62.38
	$P_{720}^{\vec{BSPTS}}$	984–1281	1077	23.21	275–359	289	23.24	121–125	125	3.56
P_{high}	$P_{15}^{\vec{TS}}$	579–1579	1033	63.33	101–359	247	71.75	42–4042	230	98.97
	$P_{60}^{\vec{BSPTS}}$	579–1579	1015	63.33	101–359	243	71.75	42–1042	157	96.00
	$P_{180}^{\vec{BSPTS}}$	579–1579	963	63.33	101–359	232	71.75	42–375	110	88.89
	$P_{360}^{\vec{BSPTS}}$	579–1579	908	63.33	101–359	212	71.75	42–208	87	80.00
	$P_{720}^{\vec{BSPTS}}$	579–1281	828	54.81	101–359	178	71.75	42–125	79	66.67

considered to be 0 W. The BSPTS has an energy buffer, which allows different demand profiles. Of note here is that the buffering is only useful if its before the demand moment, as in the case of the BSP, because only uni-directional buffer charging is allowed.

Second, we vary the power step-size P_{step}, comparable to the BSP and BS scenarios. However, for simplicity we vary between a low step-size option (P_{low}) and a high step-size option (P_{high}). P_{low} has two or three power steps, zero, P_{max}^{BSPTS} (4000 W) and the power demand the same as the specific maximum power demand of the input profile under evaluation, if this is not the same as P_{max}^{BSPTS}. Furthermore, P_{high} has a power step-size of 1% of P_{max}^{BSPTS} including the specific $P_{d}^{\vec{BSPTS}}$ profile under evaluation.

Finally, choose the two remaining parameters to be constant. First, the total energy demand E_{dem}^{BSPTS} is 1 kWh. Second, the BSPTS energy buffer E_{cap}^{BSPTS} which is the same as E_{dem}^{BSPTS}.

3.5.2. Expectations

More broadly, we expect large reductions in ESS requirements as found in [36]. With the exception of having no availability limitations, the BSPTS can been seen as combination of a BSP and a TS. Therefore, we expect the results to be similar to the BSP and TS cases. First, the results of the P_{low} scenarios should be comparable to the TS scenario, as the reduced controllability of the BSPTS buffer will provide limited flexibility to the system, comparable to the demand profile being static. However, we expect the P_{high} results to be similar to the BSP results, as the increased controllability of the BSPTS buffer will allow the ESS reduction to depend more on the buffer and less on the input profile.

3.5.3. Results

Table 5 shows the results for both the P_{low} and the P_{high} scenarios, whereby the maximum percentage reduction is in respect to the maximum ESS requirements for a specific input profile (i.e., the demand is at the beginning of the simulation period where no buffering is possible). The P_{low} ESS requirements ranges and maximum reduction percentages are identical to the TS situation (see Table 4), which is expected as the non zero power demand periods are equal. Furthermore, this means that the BSPTS internal buffer cannot be controlled sufficiently to further enhance the maximum ESS sizing reduction. However, the average ESS requirements found are higher for the BSPTS case than the TS case. This is because the BSPTS can only buffer at peak EP_{+} and cannot buffer after the demand has occurred, whereas the TS can shift the complete profile to all moments. However, the buffer is sufficient to lower the ESS requirements after for TAW including periods after midday. We conclude that more ESS sizing requirement reductions can be achieved if the demand is fully shiftable than if its only bufferable. Note this is not necessarily a fair comparison as the TS case inherently has more moments than the BSPTS case due to the TAWs shifting.

Furthermore, the internal buffer can provide more flexibility for the P_{high} scenarios, and the ESS capacity E_{cap}^{ESS} and maximum charge power P_{ch}^{ESS} ranges for all input profiles except $P_{720}^{\vec{BSPTS}}$ are identical to the BSP $\vec{P_{1\%}}$ case. However, input $P_{720}^{\vec{BSPTS}}$ enables lower maximum E_{cap}^{ESS} due to the input demand not requiring as much capacity, as the profiles is long enough to always overlap with a large EP_{+} moment. For P_{dis}^{ESS}, the minimum of the range of power is the same as the BSP situation, but the maximum range of the power is defined by the requirements of $P_{d}^{\vec{BSPTS}}$, and is comparable to the TS situation. Furthermore, the BSPTS averages for P_{ch}^{ESS} and P_{dis}^{ESS} are lower in than in the TS situation, but the E_{cap}^{ESS} averages differ per input profile if they are higher or lower.

3.5.4. Reflection

The P_{low} scenarios are indeed similar to the TS results, and the P_{high} scenarios similar to BSP with a P_{step} of 1%, as the BSPTS P_{step} is equal. Furthermore, reductions in ESS sizing comparable to [36] were found in the majority of BSPTS scenarios.

4. Discussion

The goal of this paper is to investigate the potential of using different flexible load types to reduce ESS sizes. Based on the results, we have a number of broader observations. First, by controlling flexible loads, the sizes of ESS used to handle the remaining power imbalance can be reduced. In many cases, the reduction was significant. Therefore, to avoid over-dimensioning of energy storage, local flexibility must be considered when sizing energy storage.

Second, flexible load availability at moments when a large power surplus (large EP_{+}) is available leads to the highest sizing reductions. Furthermore, even flexible load availability during a small part of a large energy surplus period can significantly reduce the ESS requirements. Conversely, if the TAW includes no part of the large energy surplus period, ESS sizing requirements are considerably larger. Therefore, reducing ESS sizing by shifting flexible loads has questionable robustness. If for example the ESS requirements are calculated considering only the large EP_{+} moments, the ESS could be considerably under-dimensioned. More generally, large EP_{+} moments for local microgrids are generally during peak solar production moments. Therefore, making flexible loads available during the day could significantly reduce ESS requirements. Furthermore, extending TAWs outside of large EP_{+} moments does not further reduce ESS sizing. Also, when a BS flexible load can discharge to the local grid, the ESS sizing can be further reduced by including large EP_{-} moments in the TAW.

Third, the ESS sizing reduction was highest (and therefore flexible loads provide the most added value) when P_{step} of the flexible load was low. This shows that a flexible load with high power controllability can provide flexibility to the local microgrid, reducing the need for ESS

flexibility to be provided. Generally, this means that in situations where flexible loads such as e-boilers are present (large P_{step}), larger ESS are required to handle the remaining local imbalance than in situations where heat pumps (small P_{step}) are present. However, this only holds if the maximum powers, buffer sizes and power demands of both the e-boiler and the heat pump are comparable.

Finally, although using BS flexibility can completely remove the need for ESS, it requires longer TAWs than BSP flexibility, as the BS must also be available when the microgrid is at an energy deficit (no local energy being produced). Although in the cases examined, maximum reduction was only achieved when the BS is available for a full day, in practice there may be peaks that should be removed, requiring a shorter BS availability. For example, evening peak demands generally found of residential microgrids could be removed, reducing the highest amount of ESS sizing for the lowest amount of BS availability.

5. Conclusions and future work

To avoid over-dimensioning of energy storage systems, we recommend considering local flexibility when sizing energy storage. When local flexible load are considered, the amount of energy storage required to handle any remaining power imbalance can be significantly decreased. However, under-dimensioning of energy storage systems is also possible if only TAWs are considered where a high surplus of energy is available locally. Additionally, we investigated the influences of several factors on the ESS reduction, including power step-size, load availability and time dependent load demand, for the four types of flexible loads. We found that for BSP and BS loads, a step-size of 10% of maximum power is sufficient to significantly reduce all storage requirements. Furthermore, a short window of availability coinciding with the largest EP_+ moment is sufficient to reduce ESS capacity and power discharge by 63.33% and 97.22% respectively. For BS loads, further reduction was possible by lengthening the availability window of the flexible load, thereby almost completely removing the need for energy storage.

Furthermore, the TS load can supply flexibility, enabling similar energy storage reductions as the BSP. However, this flexibility is less robust, as it depends on the time dependent profile of the TS. Finally, the BSPTS can provide similar flexibility to the TS if the power step-sizes are large, and flexibility similar to the BSP if power step-sizes are smaller.

For future work, we recommend furthering this research by considering the real-world constraints of both the flexible loads and the energy storage devices, to have a more practical understanding of how local flexible devices can effect storage sizing. Furthermore, we recommend investigating the effects of combining different types of flexible loads into a single system with respect to storage sizing, to see if synergies between flexible loads can be realized to further reduce ESS sizing. This investigation could be based on a residential microgrid scenario, including examining the role of a grid connection to provide further flexibility to the local grid, as well as examining the influence of interday energy storage. Finally, as only the PS heuristic was used in this research, we recommend an investigation into the influence of other control objectives, such as cost or CO2 emission minimization, on ESS sizing.

CRediT authorship contribution statement

Edmund W. Schaefer: Writing – review & editing, Writing – original draft, Visualization, Validation, Software, Resources, Methodology, Investigation, Formal analysis, Data curation, Conceptualization. **Gerwin Hoogsteen:** Writing – review & editing, Supervision, Project administration, Methodology, Funding acquisition, Conceptualization. **Johann L. Hurink:** Writing – review & editing, Supervision, Project administration, Funding acquisition. **Richard P. van Leeuwen:** Writing – review & editing, Supervision, Project administration, Funding acquisition.

Declaration of competing interest

The authors declare that they have no known competing financial interests or personal relationships that could have appeared to influence the work reported in this paper.

Data availability

Data will be made available on request.

Acknowledgements

This study is part of the SUSTENANCE project, funded by the European Union's Horizon 2020 research program under grant agreement No 101022587, and the BatteryNL project, funded by the Dutch Research Council NWO under grant agreement number NWA.1389.20.089.

Appendix. Mathematical formulations

All mathematical models based on [37]. For scheduling, algorithms are used from [38].

A.1. Energy storage systems

Energy storage systems, referred to in [37] as buffer devices, are devices which can store energy for later use. As modelled here, they do not have any inherent demands of their own, and are considered to be ideal (i.e., no efficiency losses). The relationship describing the State of Charge (SoC) of the ESS at any moment t is given Eq. (4), whereby E_{buf}^{SoC} is the SoC of the ESS, P_{buf} is the power demand of the ESS, t is the time interval of length T.

$$E_{buf}^{SoC}(t) = E_{buf}^{SoC}(t-1) + P_{buf}(t) \cdot T \tag{4}$$

Furthermore, two constraints are required. First, the SoC of the ESS must be between the minimum and maximum capacity values (E_{buf}^{min} and E_{buf}^{max} respectively), as shown in Eq. (5).

$$E_{buf}^{max} \leq E_{buf}^{SoC}(t) \leq E_{buf}^{max} \tag{5}$$

Second, P_{buf} must not exceed the SoC constraints (i.e., more energy should not be charged or discharged from the storage device than is possible). This constraint is given in Eq. (6), whereby the maximum and minimum possible ESS powers are given by P_{buf}^{max} and P_{buf}^{min} respectively.

$$\begin{aligned} P_{buf}(t)\, \epsilon\, [&\max(P_{buf}^{min}, -E_{buf}^{SoC}(t) * \frac{1}{T}), \\ &\min(P_{buf}^{max}, (E_{buf}^{max} - E_{buf}^{SoC}(t)) * \frac{1}{T})] \end{aligned} \tag{6}$$

A.2. Time shiftable devices

Time Shiftable (TS) devices, also referred to as Time Shiftable devices in [37], are devices which can shift energy consumption to later moments given a predefined load profile of N intervals. Eq. (7) shows the constraints for each possible devices state T_{state}. Here, $UNAV$ is the state in which the TS is not available for shifting, whereby $T_{TS}^{S,AV}$ is the start time of availability and $T_{TS}^{E,AV}$ is the end time availability. Next, AV is the state in which the TS is available for shifting, whereby T_{TS}^{Start} is the start time set for the demand profile. The demand profile can only be shifted over time, but once started the profile must be executed uninterrupted. Next, RUN is the state in which the demand profile is being executed, whereby $(\frac{t-T_{TS}^{Start}}{T} * N)$ is end time of the profile in

respect to the starting time T_{TS}^{Start}. Finally, $DONE$ is the state in which the profile has been executed.

$$TS_{state} = \begin{cases} UNAV, & \text{if } t < T_{TS}^{S,AV} \vee t > T_{TS}^{E,AV} \\ AV, & \text{if } T_{TS}^{S,AV} \leq t < T_{TS}^{Start} \\ RUN, & \text{if } T_{TS}^{Start} \leq t < \frac{t-T_{TS}^{Start}}{T} * N \\ DONE, & \text{if } \frac{t-T_{TS}^{Start}}{T} * N \leq t \leq T_{TS}^{E,AV} \end{cases} \tag{7}$$

A.3. Buffer shiftable and time shiftable combined

Buffer and Time Shiftable Devices (BTS), referred to as Buffer-Timeshiftable devices in [37], include the flexible device types Buffer Shiftable (BS), Buffer Shiftable Positive (BSP) and Buffer Shiftable Positive Time Shiftable (BSPTS). BTS devices are devices which can buffer energy as well as shift energy demand to later moments. They inherit all of the characteristics from Appendix A.1. Hereby, both BSP and BSPTS types have a P_{buf}^{min} of 0 (i.e., no export from buffer to microgrid is possible) while a BS has a value which is less than 0 (i.e., export is possible).

In addition, BTS devices have similar time constrained states to those presented in Appendix A.2. However, the BTS can only be in one of two states, available or unavailable, see Eq. (8). First, the $UNAV$ state, where the devices is unavailable for buffering, whereby $T_{BTS}^{S,AV}$ is the start moment of availability of the BTS and $T_{BTS}^{S,AV}$ is the end moment of availability. Second, the AV state, where the devices are available for energy buffering. Hereby both BS and BSP types have limited availability, and the BSPTS type has availability which is equal to the entire period under investigation (i.e., the $UNAV$ state never occurs in this work).

$$BTS_{state} = \begin{cases} UNAV, & \text{if } t < T_{BTS}^{S,AV} \vee t > T_{BTS}^{E,AV} \\ AV, & \text{if } T_{BTS}^{S,AV} \leq t < T_{BTS}^{E,AV} \end{cases} \tag{8}$$

Finally, for all BTS devices a target buffer value must be satisfied, see Eq. (9). Hereby $E_{BTS}^{SOC}(\tau)$ is the SoC of the BTS, $E_{BTS}^{des}(\tau)$ is the desired SoC of the BTS, both at moment τ, which in this work is considered to be the end time of the availability window.

$$E_{BTS}^{SOC}(\tau) = E_{BTS}^{des}(\tau) \tag{9}$$

References

[1] Quality of electricity supply - country ranking 2019 | Statista — statista.com, 2024, https://www.statista.com/statistics/268155/ranking-of-the-20-countries-with-the-highest-quality-of-electricity-supply/, [(Accessed 31 January 2024)].

[2] Netcongestie: waarom beland je als bedrijf op een wachtlijst? — ondernemen.nl, 2024, https://www.ondernemen.nl/artikelen/netcongestie-waarom-beland-je-als-bedrijf-op-een-wachtlijst, [(Accessed 31 January 2024)].

[3] Enexis ziet druk op elektriciteitsnet ook in woonwijken toenemen — enexisgroep.nl, 2024, https://www.enexisgroep.nl/nieuws/enexis-ziet-druk-op-elektriciteitsnet-ook-in-woonwijken-toenemen, [(Accessed 31 January 2024)].

[4] E. Lannoye, D. Flynn, M. O'Malley, Evaluation of power system flexibility, IEEE Trans. Power Syst. 27 (2) (2012) 922–931.

[5] A. Ulbig, G. Andersson, Analyzing operational flexibility of electric power systems, Int. J. Electr. Power Energy Syst. 72 (2015) 155–164, The Special Issue for 18th Power Systems Computation Conference..

[6] P. Mandatova, Mikhailova, Flexibility and Aggregation - Requirements for Their Interaction in the Market, Tech. Rep., EURELECTRIC, 2014, https://www.iene.eu/eurelectric-publication-flexibility-and-aggregation-requirements-for-their-interaction-in-the-market-p296.html, (Accessed 05 February 2024).

[7] A. Ulbig, G. Andersson, Chapter 18 - role of power system flexibility, in: L.E. Jones (Ed.), Renewable Energy Integration, Academic Press, Boston, 2014, pp. 227–238.

[8] M.M. Rana, M. Uddin, M.R. Sarkar, S.T. Meraj, G. Shafiullah, S. Muyeen, M.A. Islam, T. Jamal, Applications of energy storage systems in power grids with and without renewable energy integration — A comprehensive review, J. Energy Storage 68 (2023) 107811.

[9] S. Aggarwal, R. Orvis, Grid Flexibility: Methods for Modernizing the Power Grid, Tech. Rep., Energy Innovation, San Francisco, 2016.

[10] M. Yekini Suberu, M. Wazir Mustafa, N. Bashir, Energy storage systems for renewable energy power sector integration and mitigation of intermittency, Renew. Sustain. Energy Rev. 35 (2014) 499–514.

[11] B. Homan, Batteries in Smart Microgrids (Ph.D. thesis), in: IDS Ph.D. Thesis Series, (2020–001) University of Twente, Netherlands, 2020.

[12] P. Warren, A review of demand-side management policy in the UK, Renew. Sustain. Energy Rev. 29 (2014) 941–951.

[13] L.A. Wong, V.K. Ramachandaramurthy, P. Taylor, J. Ekanayake, S.L. Walker, S. Padmanaban, Review on the optimal placement, sizing and control of an energy storage system in the distribution network, J. Energy Storage 21 (2019) 489–504.

[14] P. Malysz, S. Sirouspour, A. Emadi, An optimal energy storage control strategy for grid-connected microgrids, IEEE Trans. Smart Grid 5 (4) (2014) 1785–1796.

[15] Ayesha, M. Numan, M.F. Baig, M. Yousif, Reliability evaluation of energy storage systems combined with other grid flexibility options: A review, J. Energy Storage 63 (2023) 107022.

[16] I. Mahmud, M.B. Medha, M. Hasanuzzaman, Global challenges of electric vehicle charging systems and its future prospects: A review, Res. Transp. Bus. Manage. 49 (2023) 101011.

[17] T.U. Solanke, V.K. Ramachandaramurthy, J.Y. Yong, J. Pasupuleti, P. Kasinathan, A. Rajagopalan, A review of strategic charging–discharging control of grid-connected electric vehicles, J. Energy Storage 28 (2020) 101193.

[18] A. Heider, F. Moors, G. Hug, The influence of smart charging and V2G on the flexibility potential and grid expansion needs of german distribution grids, in: 2023 International Conference on Smart Energy Systems and Technologies, SEST, 2023, pp. 1–6.

[19] K. Mahmud, S. Morsalin, Y.R. Kafle, G.E. Town, Improved peak shaving in grid-connected domestic power systems combining photovoltaic generation, battery storage, and V2G-capable electric vehicle, in: 2016 IEEE International Conference on Power System Technology, POWERCON, 2016, pp. 1–4.

[20] B. Nijenhuis, J. Reuling, G. Hoogsteen, J. Hurink, The potential of indicating energy flexibility information by EV users for application in energy management systems: a dutch case study, in: 2023 IEEE International Conference on Communications, Control, and Computing Technologies for Smart Grids (SmartGridComm), 2023, pp. 1–6.

[21] A. Arteconi, N. Hewitt, F. Polonara, Domestic demand-side management (DSM): Role of heat pumps and thermal energy storage (TES) systems, Appl. Therm. Eng. 51 (1) (2013) 155–165.

[22] A. Arteconi, F. Polonara, Assessing the demand side management potential and the energy flexibility of heat pumps in buildings, Energies 11 (7) (2018).

[23] S. Zator, W. Skomudek, Impact of DSM on energy management in a single-family house with a heat pump and photovoltaic installation, Energies 13 (20) (2020) URL https://www.mdpi.com/1996-1073/13/20/5476.

[24] M.E.T. Gerards, J.L. Hurink, On the value of device flexibility in smart grid applications, in: 2017 IEEE Manchester PowerTech, 2017, pp. 1–6.

[25] S. Dorahaki, M. Rashidinejad, S.F. Fatemi Ardestani, A. Abdollahi, M.R. Salehizadeh, A home energy management model considering energy storage and smart flexible appliances: A modified time-driven prospect theory approach, J. Energy Storage 48 (2022) 104049.

[26] Y. Wang, W. Saad, N.B. Mandayam, H.V. Poor, Load shifting in the smart grid: To participate or not? IEEE Trans. Smart Grid 7 (6) (2016) 2604–2614.

[27] Y. Yang, S. Bremner, C. Menictas, M. Kay, Battery energy storage system size determination in renewable energy systems: A review, Renew. Sustain. Energy Rev. 91 (2018) 109–125.

[28] R. Khezri, A. Mahmoudi, M.H. Haque, A demand side management approach for optimal sizing of standalone renewable-battery systems, IEEE Trans. Sustain. Energy 12 (4) (2021) 2184–2194.

[29] Y. Ding, Q. Xu, Y. Huang, Optimal sizing of user-side energy storage considering demand management and scheduling cycle, Electr. Power Syst. Res. 184 (2020) 106284.

[30] R. Atia, N. Yamada, Sizing and analysis of renewable energy and battery systems in residential microgrids, IEEE Trans. Smart Grid 7 (3) (2016) 1204–1213.

[31] M.K. Kiptoo, O.B. Adewuyi, H.O.R. Howlader, A. Nakadomari, T. Senjyu, Optimal capacity and operational planning for renewable energy-based microgrid considering different demand-side management strategies, Energies 16 (10) (2023).

[32] P. Mirhoseini, N. Ghaffarzadeh, Economic battery sizing and power dispatch in a grid-connected charging station using convex method, J. Energy Storage 31 (2020) 101651.

[33] K. Lappalainen, J. Kleissl, Sizing of stationary energy storage systems for electric vehicle charging plazas, Appl. Energy 347 (2023) 121496.

[34] C. Essayeh, T. Morstyn, Optimal sizing for microgrids integrating distributed flexibility with the Perth West smart city as a case study, Appl. Energy 336 (2023) 120846.

[35] M. Ali, J. Ekström, M. Lehtonen, Sizing hydrogen energy storage in consideration of demand response in highly renewable generation power systems, Energies 11 (5) (2018) URL https://www.mdpi.com/1996-1073/11/5/1113.

[36] U. Mulleriyawage, W. Shen, Impact of demand side management on optimal sizing of residential battery energy storage system, Renew. Energy 172 (2021) 1250–1266.

[37] G. Hoogsteen, A Cyber-Physical Systems Perspective on Decentralized Energy Management first ed., (Ph.D. thesis), in: CTIT Ph.D. thesis series, (17–449) University of Twente, Netherlands, 2017.
[38] T. van der Klauw, Decentralized Energy Management with Profile Steering – Resource Allocation Problems in Energy Management (Ph.D. thesis), (CTIT Ph.D. thesis Series No. 17-424) University of Twente, PO Box 217, 7500 AE Enschede, The Netherlands, 2017.
[39] B. Nijenhuis, L. Winschermann, N. Arias, G. Hoogsteen, J. Hurink, Protecting the distribution grid while maximizing EV energy flexibility with transparency and active user engagement, in: CIRED Porto Workshop 2022: E-Mobility and Power Distribution Systems, 2022.
[40] University of Twente, Profile steering software, 2024, URL https://github.com/utwente-energy/profilesteering/.https://github.com/utwente-energy/profilesteering/, (Accessed 12 January 2024).
[41] E. Schaefer, G. Hoogsteen, J. Hurink, R. van Leeuwen, Sizing of hybrid energy storage through analysis of load profile characteristics: A household case study, J. Energy Storage 52 (2022) 104768.
[42] E.W. Schaefer, G. Hoogsteen, B. Nijenhuis, J.L. Hurink, R.P.v. Leeuwen, The effect of data resolution on the sizing of energy storage systems using a load profile signal decomposition method, in: 2023 IEEE International Conference on Communications, Control, and Computing Technologies for Smart Grids, SmartGridComm, 2023, pp. 1–6.
[43] L.S. Athanasiou, D.I. Fotiadis, L.K. Michalis, 8 - propagation of segmentation and imaging system errors, in: L.S. Athanasiou, D.I. Fotiadis, L.K. Michalis (Eds.), Atherosclerotic Plaque Characterization Methods Based on Coronary Imaging, Academic Press, Oxford, 2017, pp. 151–166.